

Emissivity characteristics of roughened aluminum alloy surfaces and assessment of multispectral radiation thermometry (MRT) emissivity models

Chang-Da Wen, Issam Mudawar *

*Boiling and Two-Phase Flow Laboratory, School of Mechanical Engineering, Purdue University,
1288 Mechanical Engineering Building, West Lafayette, IN 47907-1288, USA*

Received 17 March 2004; received in revised form 30 April 2004

Abstract

Experiments were performed to examine the emissivity characteristics of aluminum alloy samples over the spectral range of 2.05 to 4.72 μm and temperatures of 600, 700 and 800 K. AL 1100, 7150, 7075 and 2024 samples were tested which possessed polished, 6- and 14- μm surface finishes. Additionally, extruded and saw-cut samples were tested to examine the effects of extreme roughness on emissivity. For the polished, 6- and 14- μm samples, the emissivity decreased appreciably between 2.05 and 3.5 μm , and increased slightly between 3.5 and 4.72 μm . Spectral variations were far less pronounced for the extruded and saw-cut surfaces. Eighteen MRT emissivity models were examined for accuracy in temperature measurement. Drastic changes in the emissivity distribution precluded the use of a single function to accurately represent every band of the measured spectrum. Overall, two relatively simple models provided the best overall predictions for different alloys and temperatures. These are the same models that yielded the best overall results for polished aluminum surfaces in a previous study by the authors. Despite the relative success of these models, this study points to a need to greatly enhance the measurement accuracy of radiation thermometers to meet the needs of the aluminum industry.

© 2004 Elsevier Ltd. All rights reserved.

1. Introduction

Although steel remains the most popular alloy in most heavy industries, the past few decades have witnessed a gradual shift in favor of aluminum alloys. This shift has been brought about by many attractive attributes of aluminum including high strength-to-weight ratio, corrosion resistance and full recyclability. Three product categories consume about 67.5% of the nearly 24 billion pounds of aluminum produced in North America: transportation (aircraft, satellites, trains and more recently aluminum-intensive vehicles), packaging

(foil and cans), and construction (domes, bridges, siding) [1].

Despite the importance of aluminum, capital expenditures in aluminum production have lagged most industries, and fabrication methods have remained virtually unchanged for decades. Nonetheless, it is widely acknowledged throughout the aluminum industry that sustained market growth is becoming increasingly dependent upon the ability to improve aluminum alloy part quality (greater strength and hardness, better corrosion resistance, and minimal distortion) and reduce production cost.

Achieving a desired microstructure, and hence the aforementioned desired attributes, relies heavily on the ability to accurately measure alloy temperature at virtually every stage of an aluminum fabrication process. This is because microstructural development is highly

* Corresponding author. Tel.: +1-765-494-5705; fax: +1-765-494-0539.

E-mail address: mudawar@ecn.purdue.edu (I. Mudawar).

Nomenclature

c_1	first thermal radiation constant
c_2	second thermal radiation constant
DWRT	dual-wavelength radiation thermometry
HRR	Hagen–Rubens emissivity model
IST	inverse spectral temperature emissivity model
IWS	inverse wavelength squared emissivity model
L_e	spectral intensity of target surface emission reflected by surroundings
L_s	spectral intensity of radiation associated with scattering and absorption
$L_{\lambda,b}$	spectral intensity of blackbody radiation
$L_{\lambda,e}$	spectral intensity of radiation emitted by target surface
$L_{\lambda,gen}$	generated spectral radiation intensity
$L_{\lambda,meas}$	measured spectral radiation intensity
$L_{\lambda,ref}$	spectral intensity of irradiation from surroundings that is reflected by target surface
LEM	linear emissivity model
LLE	log-linear emissivity model
MRT	multispectral radiation thermometry
n	number of unknown coefficients in emissivity model

N	minimum number of wavelengths required in MRT model
Ra	arithmetic average roughness
SRT	spectral radiation thermometry
T	surface temperature
T_{sur}	temperature of surroundings
T_λ	spectral radiance temperature
WLT	wavelength temperature emissivity model

Greek symbols

ε_λ	spectral emissivity
λ	wavelength
ρ_λ	spectral reflectivity

Subscripts

b	blackbody
e	emitted
gen	generated
meas	measured
ref	reflected
sur	surroundings
λ	spectral

temperature dependent. Different types of temperature sensors are used in the aluminum industry, including direct contact probes and radiation thermometers. While they are still widely used, direct contact thermocouples and thermistors can mar the aluminum surface, besides being difficult to implement with parts in fast transit (e.g. extrusions), where temperature measurement accuracy is limited to ± 10 to 25 K [2].

Radiation thermometry is the method of choice for temperature measurement of fast-moving aluminum surfaces. It is a convenient non-contact method that utilizes the spectral intensity of thermal radiation from the target surface to infer surface temperature. Four components contribute to the spectral intensity, $L_{\lambda,meas}$, measured by a radiation thermometer,

$$L_{\lambda,meas}(\lambda, T) = L_{\lambda,e}(\lambda, T) + L_{\lambda,ref} + L_e + L_s, \quad (1)$$

where $L_{\lambda,e}$, $L_{\lambda,ref}$ and L_e are the intensities of radiation emitted from the target, irradiation from the surroundings reflected by the target surface, target emission reflected by the surroundings and then the target itself, respectively, and L_s is the combined effect of atmospheric scattering and absorption (H_2O , CO_2 , dust particles, etc).

The measured intensity is referenced to that of a perfect absorber and perfect emitter, blackbody, whose spectral intensity is given by the Planck distribution.

$$L_{\lambda,b}(\lambda, T) = \frac{c_1}{\lambda^5 (e^{c_2/\lambda T} - 1)}, \quad (2)$$

where $c_1 = 1.19 \times 10^8 \text{ W } \mu\text{m}^4 \text{ m}^{-2} \text{ sr}^{-1}$ and $c_2 = 1.439 \times 10^4 \text{ } \mu\text{m K}$.

Spectral emissivity, ε_λ , is the ratio of intensity of radiation emitted by a real surface to that by a blackbody at the same temperature,

$$\varepsilon_\lambda(\lambda, T) = \frac{L_{\lambda,e}(\lambda, T)}{L_{\lambda,b}(\lambda, T)}. \quad (3)$$

If the target area is small relative to its surroundings, the surroundings behave as a large blackbody enclosure that is capable of absorbing all incoming radiation, and the term L_e in Eq. (1) can be neglected. The atmospheric scattering term L_s is significant only over narrow wavelength bands and negligible elsewhere. Excluding those atmospheric scattering bands, the intensity of radiation measured from an opaque surface can be simplified as

$$\begin{aligned} L_{\lambda,meas}(\lambda, T) &\cong L_{\lambda,e}(\lambda, T) + L_{\lambda,ref} \\ &= \varepsilon_\lambda L_{\lambda,b}(\lambda, T) + \rho_\lambda L_{\lambda,b}(\lambda, T_{sur}), \end{aligned} \quad (4)$$

where ρ_λ is the spectral reflectivity of the target surface, which is the fraction of intensity of irradiation from the surroundings (at T_{sur}) that is reflected by the target surface. For a diffuse opaque surface, Kirchhoff's law

and energy conservation yield $\rho_\lambda = 1 - \varepsilon_\lambda$. This leads to the following popular expression for the measured radiation intensity of an opaque target surface,

$$L_{\lambda,\text{meas}}(\lambda, T) = \varepsilon_\lambda L_{\lambda,\text{b}}(\lambda, T) + (1 - \varepsilon_\lambda) L_{\lambda,\text{b}}(\lambda, T_{\text{sur}}). \quad (5)$$

Knowing ε_λ , Eq. (5) enables the determination of target surface temperature T from the measured spectral intensity. This equation can be further simplified by neglecting the second right-hand-side term where the surface temperature far exceeds that of the surroundings (i.e. $L_{\lambda,\text{b}}(\lambda, T) \gg L_{\lambda,\text{b}}(\lambda, T_{\text{sur}})$). While this is a reasonable assumption for measurements made in a controlled laboratory environment, caution must be exercised in adopting the same simplification in a commercial aluminum production environment where the target surface may be surrounded by several high-temperature irradiation sources.

Three main categories of radiation thermometry methods are widely used which utilize Eq. (5) to infer surface temperature: spectral, dual-wavelength and multispectral. Spectral radiation thermometry (SRT) utilizes intensity measurement at a single wavelength and a constant emissivity value to determine the surface temperature. Dual-wavelength radiation thermometry (DWRT) requires intensity measurements at two wavelengths coupled with an emissivity compensation algorithm to infer the surface temperature. Multispectral radiation thermometry (MRT) employs intensity measurements at three or more wavelengths in conjunction with a multiwavelength emissivity model to infer the surface temperature. Because of their inability to capture the complex spectral emissivity behavior of aluminum alloy surfaces, the spectral and dual-wavelength methods have been shown to yield unacceptable errors in surface temperature measurement [3]. This is why recent studies, including the present, have been focused mostly on the MRT method.

Regardless of the method used, Eq. (5) shows accurate temperature measurement requires a thorough understanding of the spectral emissivity characteristics of the target surface. The emissivity models used in Eq. (5) to determine surface temperature consist of either analytical functions based on fundamental physical premises (e.g., Maxwell, Hagen–Rubin, and Edwards models [4,5]), or mathematical functions whose coefficients are empirically determined from radiation intensity measurements at different wavelengths. By adjusting coefficient values in both types of models, the MRT method is highly effective at capturing the complex spectral emissivity characteristics of different surface materials and textures.

The *exact technique* and the *least-squares technique* are two mathematical methods used in MRT to infer surface temperature. The exact technique employs an emissivity model with n unknown coefficients and radiation intensity measurements at $n + 1$ wavelengths.

Applying Eq. (5) results in $n + 1$ equations with $n + 1$ unknowns: the target surface temperature, T , and the n unknown coefficients of the emissivity model. The least-squares technique consists of fitting radiation intensity data for several wavelengths to simultaneously infer the spectral emissivity and temperature of the target surface. This technique overcomes the relatively large, *over-fitting* errors of the exact technique when used with more than three wavelengths [6]. When using an emissivity model with n unknown coefficients, the least-squares technique requires spectral intensity measurements at a minimum of $N = n + 2$ wavelengths.

The least-squares technique enables the simultaneous determination of both the surface temperature and unknown emissivity coefficients by minimizing the magnitude of

$$\chi^2 = \sum_{i=0}^n (L_{\lambda,\text{meas},i} - L_{\lambda,\text{gen},i})^2, \quad (6)$$

where $L_{\lambda,\text{meas},i}$ is the measured spectral intensity and $L_{\lambda,\text{gen},i}$ the intensity value generated according to the following equation

$$L_{\lambda,\text{gen}}(\lambda, T) \cong \varepsilon_\lambda(\lambda) L_{\lambda,\text{b}}(\lambda, T) = \varepsilon_\lambda(\lambda) \frac{c_1}{\lambda^5 (e^{c_2/\lambda T} - 1)}. \quad (7)$$

For emissivity models with exponential form, a modified linear least-squares technique is used, which consists of minimizing the magnitude of

$$\chi^2 = \sum_{i=0}^n (\ln L_{\lambda,\text{meas},i} - \ln L_{\lambda,\text{gen},i})^2, \quad (8)$$

where the Planck distribution used to determine $L_{\lambda,\text{gen},i}$ is approximated by

$$L_{\lambda,\text{b}}(\lambda, T) = \frac{c_1}{\lambda^5 (e^{c_2/\lambda T} - 1)} \cong \frac{c_1}{\lambda^5 (e^{c_2/\lambda T})}. \quad (9)$$

This procedure results in a set of equations that are linear with respect to temperature and the unknown emissivity coefficients.

Aluminum alloys pose serious challenges to the implementation of radiation thermometry for several reasons. First, the low emissivity of aluminum surfaces produces inherently weak intensity signals. Also, high reflectivity increases measurement sensitivity to irradiation from the surroundings, which, in a commercial aluminum production environment, may include several high-temperature sources of irradiation. Moreover, there are no reliable databases that encompass the complex emissivity characteristics of aluminum surfaces relative to wavelength, temperature, alloy, surface finish, thermal history, and environment. Fig. 1 illustrates the complex emissivity characteristics of commercially pure aluminum (AL 11XX series) resulting from temperature and surface roughness variations.

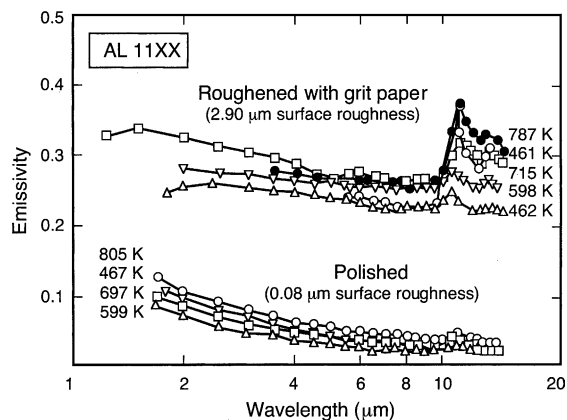


Fig. 1. Spectral emissivity of AL 11XX (adapted from Refs. [7,8]).

These challenges have led to significant difficulties in implementing MRT, let alone other less accurate methods in the aluminum industry. Previous studies have shown few aluminum emissivity models are suitable for implementation in the MRT least-squares technique, and those are valid only within specific spectral ranges [9–11].

This paper is the second of a two-part study concerning the complex emissivity characteristics of aluminum alloy surfaces. The first part [12] explored the interdependent parametric influences of temperature, heating time, and alloy on the spectral emissivity of aluminum alloys. Eighteen MRT emissivity models were examined for accuracy in temperature determination of polished aluminum surfaces. It was shown the drastic changes in the shape of emissivity distribution preclude the use of a single function to accurately represent every band of the measured spectrum. Better predictions were achieved using the simplest form of MRT emissivity models and minimum number of wavelengths required by the model. The present study explores the same parametric influences for rough aluminum alloy surfaces. A comprehensive experimental study of these influences is first discussed. Then the same 18 emissivity models are examined for suitability to predicting the temperature of rough aluminum surfaces.

2. Experimental methods

2.1. Aluminum specimens

Test samples were fabricated from four aluminum alloys, AL 1100, AL 7150, AL 7075 and AL 2024. AL 1100, which contains a minute amount of copper, is non-heat treatable and often sold as commercially pure aluminum. It is used in this study as a reference

for the other alloys. AL 7150 (6.4% Zn, 2.4% Mg, 2.2% Cu and 0.12% Zr) and AL 7075 (5.6% Zn, 2.5% Mg, 1.6% Cu and 0.23% Cr) are found mostly in aerospace structures. AL 2024 (4.4% Cu, 1.5% Mg and 0.6% Mn) has a broad range of applications, including aerospace structures, truck wheels and window frames.

Five types of surface finishes were examined: polished, 6- μm roughened, 14- μm roughened, extruded and saw-cut. Fig. 2a–e shows representative 3D images and surface profiles for each of the surface finishes applied to AL 7075 samples. The polished sample was prepared by using a series of five polishing wheels with increasing finer grit and particle size (320 grit SiC, 400 grit SiC, 600 grit SiC, diamond, Gamma alumina); the finishing alumina wheel produced a mechanically mirror polished surface with roughness features smaller than 0.05 μm . The 6- and 14- μm finishes were achieved with a 6- μm diamond compound and a 600 Carborundum grit paper, respectively. Extrusions are formed by pressing a billet through a die to produce long parts with a uniform cross-section. The extruded samples were cut from the surface of a large extrusion, and possessed directional properties as depicted in Fig. 2d. The saw-cut samples were cut from aluminum bar and their average surface roughness was 4–12 μm across and 0.15–2.14 μm along the sawing direction. The extruded and saw-cut samples were supplied directly from the Aluminum Company of America (ALCOA) and machined to the desired specimen size for testing using extreme care to preserve their original surface finish.

2.2. Test facility

The desired surface temperature was achieved by attaching the aluminum sample to a heating block facing the spectrometer (radiation thermometer). The construction of the heating block is illustrated in Fig. 3. Using a solid thermally insulating flange made from low conductivity alumina silicate, the test sample was pressed against one of the outer flat surfaces of a large aluminum block with octagonal cross-section. The large block was heated with four cartridge heaters whose power was manually adjusted with the aid of a variable voltage transformer. The heating assembly was wrapped in high-temperature Cotronics ceramic fiber insulation. A two-dimensional translation stage was used to accurately position the sample surface relative to the spectrometer.

Fig. 4 illustrates the detailed construction of the test sample and insulating flange. The test sample surface area measures 15 mm \times 15 mm. A Chromel-Alumel (type K) thermocouple was embedded in a hole that was drilled from the top of the sample to a distance of 1 mm behind the surface. Because of the high thermal conductivity of aluminum and low heat flux supplied to the sample from the heating block, the temperature gradient

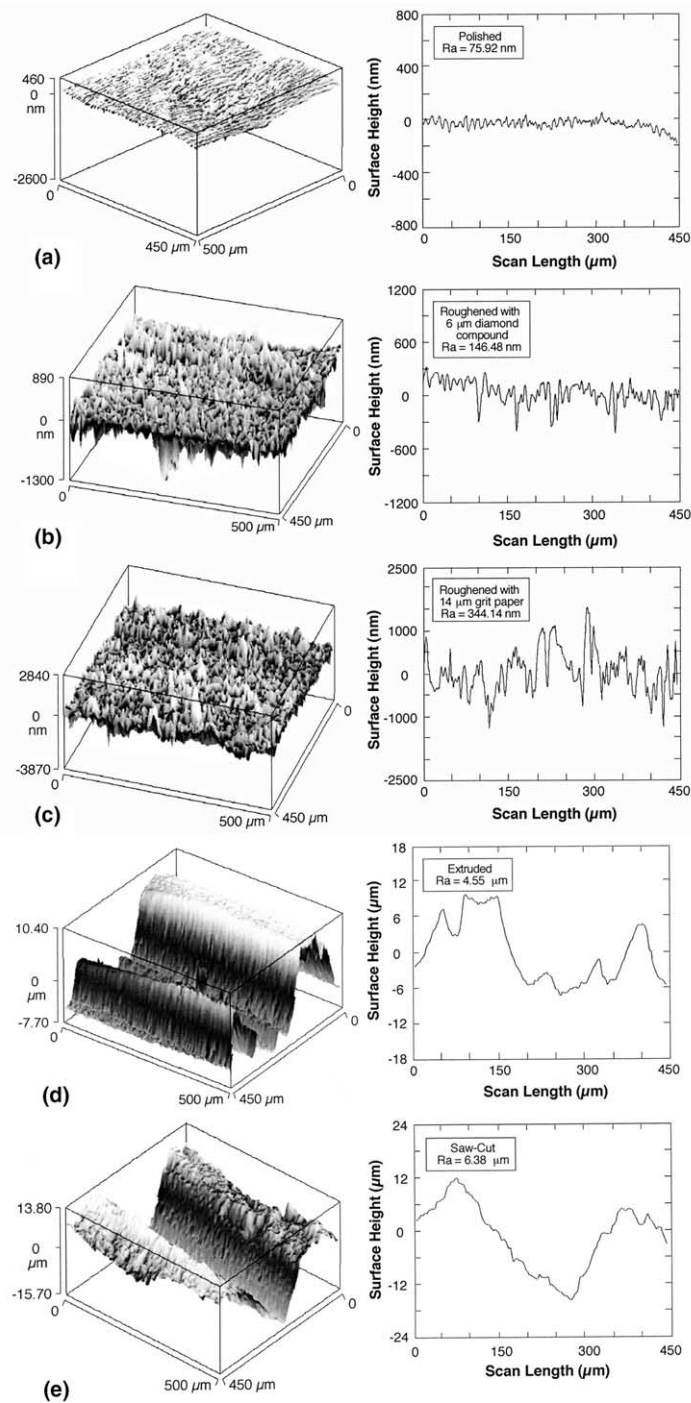


Fig. 2. 3D images and surface profiles of AL 7075 samples: (a) polished, (b) roughened with 6 μm diamond compound, (c) roughened with 14 μm grit paper, (d) extruded, and (e) saw-cut.

between the thermocouple bead and test surface was less than 0.03 K. The thermocouple was calibrated using an

Omega CL1000 hot point calibrator and had a maximum offset of 1.6 K at 523 K.

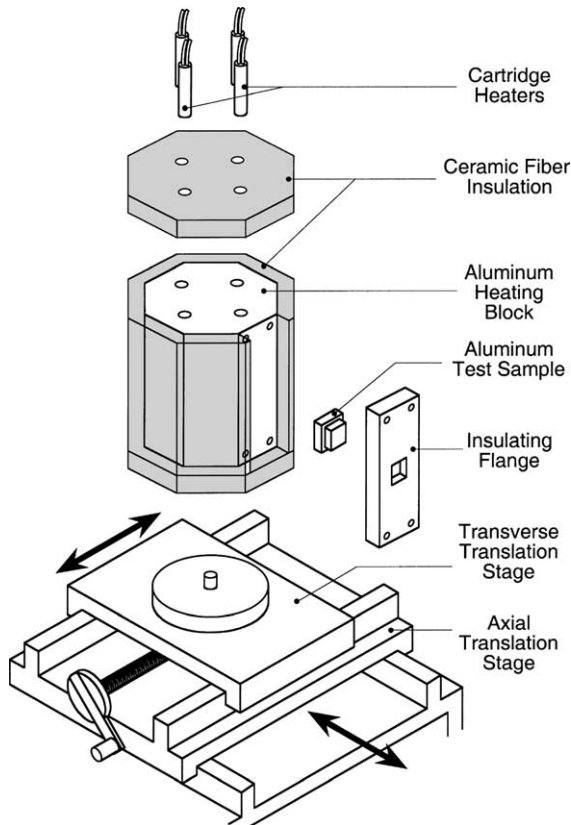


Fig. 3. Construction of sample heating assembly.

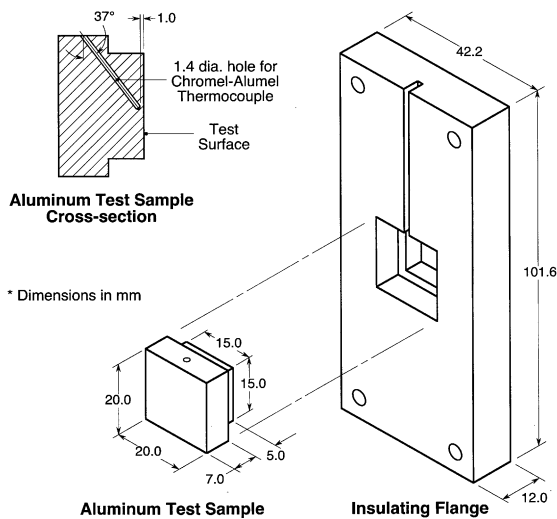


Fig. 4. Schematic diagram of aluminum test sample and insulating flange.

The radiation intensity measurements were made with a Spectraline ES100 Fast Infrared Array Spec-

trimeter (FIAS) which was carefully aligned relative to the target surface with the aid of a He-Ne laser. The FIAS is capable of measuring 160 simultaneous spectral radiation intensities for discrete wavelengths ranging from 1.8 to 4.9 μm . The incident radiation is split into spectral components that are dispersed over a staggered 160 element linear array Pb-Se detector.

2.3. Experimental procedure

After machining the sample and creating its specific surface finish, the test surface was cleaned with acetone and methanol to remove any oils, grease or dirt. The sample was handled with great care and wrapped in fine tissue to preserve the surface finish.

Three temperatures, 600, 700 and 800 K, were selected for measurement and analysis. The measurements were performed in a controlled laboratory environment with a fairly constant room temperature of about 295 K.

Before heating the AL sample, the heating block was pre-heated to a temperature slightly above the desired value. At the same time, the thermocouple was inserted into the sample. The thermocouple hole was pre-packed with high thermal conductivity boron nitride powder to ensure good thermal contact between the thermocouple bead and the sample. The sample was attached to the outer surface of the pre-heated block with the aid of the insulating flange. The desired sample temperature was achieved by fine-tuning power input to the cartridge heaters from the voltage transformer. The spectrometer was aligned by aiming a He-Ne laser beam at the center of the sample surface. Once the sample reached the desired temperature, the spectral intensity data were collected and stored at 390 Hz.

3. Results and discussion

Spectral emissivity measurements were obtained for each of the four aluminum alloys and five aforementioned surface finishes subject to variations in temperature, composition and heating time. Extruded surfaces were provided from ALCOA for AL 7150, 7075 and 2024, and saw-cut surfaces for only AL 7075 and 2024. Results for the polished surface have been presented in a previous paper by the authors [12], and will not be detailed in the present paper.

Spectral emissivity values were determined from Eq. (5), using the spectral emissivity measured by the spectrometer, $L_{\lambda, \text{meas}}$, and the blackbody intensity values $L_{\lambda, b}(\lambda, T)$ and $L_{\lambda, b}(\lambda, T_{\text{sur}})$ corresponding to the sample surface, T , and room temperature, T_{sur} , respectively. This section will discuss the parametric effects of sample temperature, heating time, alloy and surface roughness on spectral emissivity.

3.1. Temperature effects

Fig. 5 shows spectral emissivity distributions for $2 < \lambda < 4.72 \mu\text{m}$ for AL 1100, 7150, 7075 and 2024 samples with different surface finishes at 600, 700 and 800 K. The two shaded regions in each plot correspond to bands of appreciable atmospheric absorption and scattering. The first band (centered at $2.7 \mu\text{m}$) is influenced by H_2O (room humidity) and CO_2 molecules, and the other (centered at $4.3 \mu\text{m}$) by CO_2 molecules alone. Data obtained in these bands were excluded from the present assessment of emissivity models due to the appreciable error they contribute to radiation intensity.

Fig. 5 shows general similarities among the emissivity spectra for the polished, 6- and 14- μm samples. At 600 K, the emissivity decreases appreciably with increasing wavelength until $3.5 \mu\text{m}$ and increases slightly thereafter. The emissivity variations are less pronounced at 700 and 800 K. For all three temperatures, the extruded and saw-cut surfaces exhibit the expected trend for most metallic surfaces in the infrared range of monotonically decreasing emissivity with increasing wavelength.

Fig. 6 shows the effects of temperature on spectral emissivity at $\lambda = 3.5 \mu\text{m}$ for different surface finishes and alloys. The trend depicted in this figure is contrary to that of most metallic surface, whose emissivity typically increases with increasing temperature [13]. Fig. 6 shows the spectral emissivity of AL 7150, 7075 and 2024 mostly decreases between 600 and 700 K and then increases above 700 K. Physical changes to the surface at 800 K are believed to be a primary cause for the increased emissivity at this temperature. These changes were

accompanied by marked changes in surface color, from light metallic gray at 600 and 700 K to black at 800 K. This discoloration is common to aluminum alloys which contain magnesium [14], including AL 7150, 7075 and 2024. Fig. 6 also shows emissivity is generally lowest for polished samples and increases with increasing roughness.

3.2. Effects of heating time

Fig. 7 shows the effects of heating time on spectral emissivity at $\lambda = 3.5 \mu\text{m}$ and $T = 700 \text{ K}$ over a 10-h period. All alloys show slight changes in emissivity with heating time, which is consistent with trends reported by previous authors [9,10]. These changes, which occurred during the first 4 h, are attributed to oxidation growth [10,15], which is beyond the scope of the present study. Following this initial period, emissivity becomes fairly constant, which points to the surface oxidation becoming fully developed.

3.3. Effects of alloy composition

The complex effects of alloy on spectral emissivity are depicted in Fig. 8 for different surface finishes and different temperatures. In general, emissivity spectra for different alloys at a given temperature are very similar in shape but not in magnitude. As discussed earlier, surface oxidation, which is alloy dependent, can have a significant effect on emissivity. Variations in the concentration of alloying elements cause different types and degrees of oxidation, yielding measurable variations in emissivity

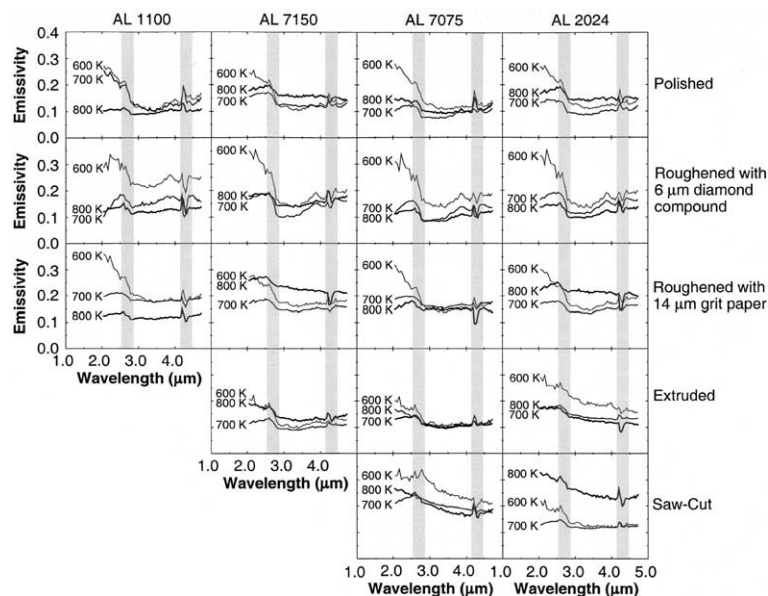


Fig. 5. Effects of temperature on spectral emissivity.

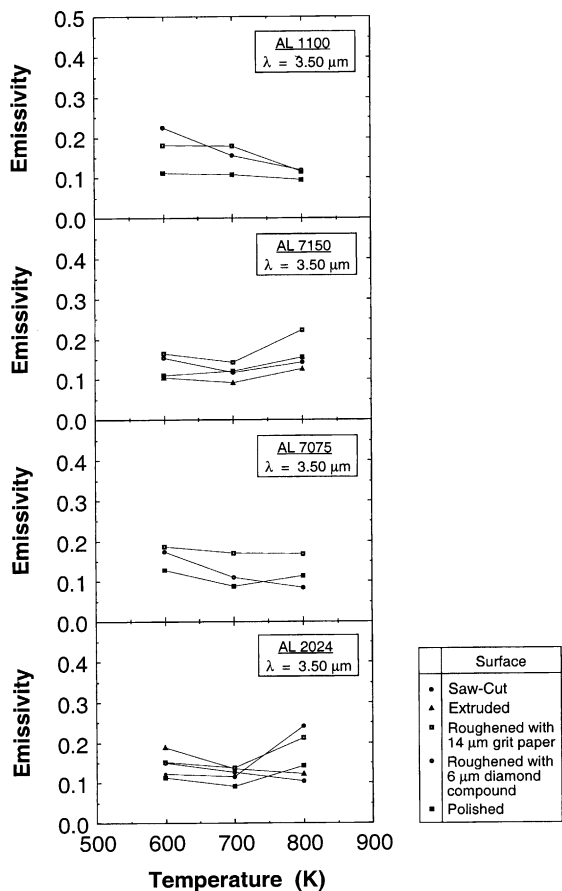


Fig. 6. Effects of temperature on spectral emissivity at 3.5 μm.

between alloys. Fig. 8 shows emissivity variations among alloys are far more pronounced at 800 K than at 600 or 700 K, and these variations generally increase with increasing surface roughness.

3.4. Effects of surface roughness

Fig. 9 depicts the effects of surface roughness on spectral emissivity. In general, the polished surface has the lowest emissivity and the saw-cut the highest. There is also an obvious difference between the shape of emissivity distributions for the polished, 6- and 14-μm surfaces, on one hand, and the extruded and saw-cut on the other. For the first three, emissivity first decreases appreciably to around 3.5 μm before increasing slightly again. For the extruded and saw-cut surfaces, the emissivity decreases monotonically with increasing wavelength, as reported in an earlier study by Pellerin [3].

The results shown in Figs. 5–9 demonstrate the highly complex emissivity behavior of aluminum alloys, and highlight the challenges in developing a universal

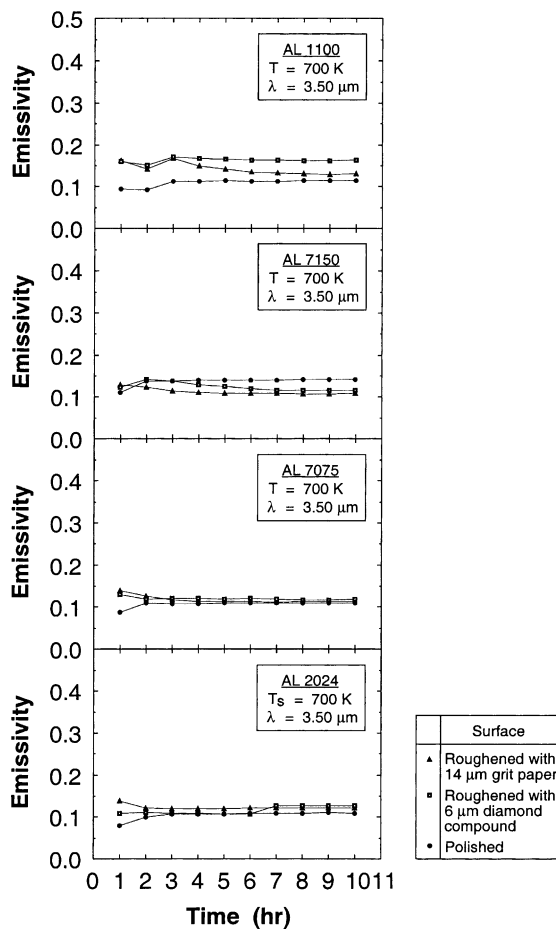


Fig. 7. Effects of heating time on spectral emissivity.

emissivity model that can be widely adopted in the aluminum industry.

4. Application of MRT emissivity models

The least-squares technique described earlier was used in the present study to simultaneously determine the surface temperature and values of coefficients in the emissivity model. The least-squares technique requires the number of measured spectral intensity values to be at least two greater than the number of unknown coefficients in the emissivity model. Table 1 shows the 18 MRT emissivity models that were examined in the present study. They encompass both mathematical functions (e.g., LLE and LEM) and analytical relations (e.g., HRR), and include 10 basic functional forms, and variations thereof based on the number of unknown coefficients used. Models 6, 7-1, 7-2, 8-1, and 8-2 are based on a spectral radiance temperature, T_s , which is

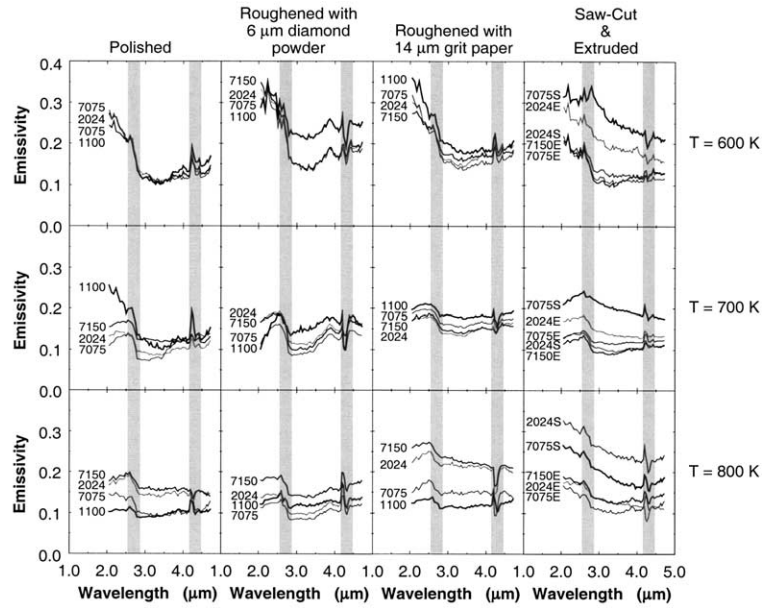


Fig. 8. Effects of alloy on spectral emissivity.

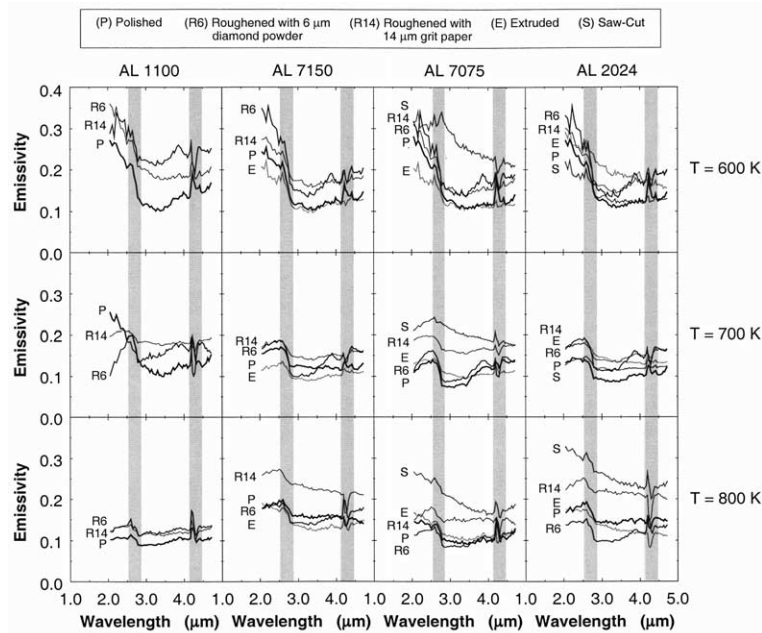


Fig. 9. Effects of surface roughness on spectral emissivity.

defined as the equivalent blackbody temperature of the measured spectral intensity.

Because of the strong discoloration phenomenon at 800 K discussed earlier, only 600 and 700 K data are included in the assessment of emissivity models. Fur-

thermore, the 14- μm surface was selected for this assessment because it represents a middle-range roughness value between polished and 6 μm surfaces on one hand and the highly roughened extruded and saw-cut surfaces on the other. Furthermore, as indicated in

Table 1
Mathematical form of emissivity models examined in this study

Emissivity model	Mathematical function	Emissivity model	Mathematical function
1-1 ^a	$\varepsilon_\lambda = \exp(a_0 + a_1\lambda)$	6 ^b	$\varepsilon_\lambda = \exp(a_0\lambda + a_1/T_\lambda)^c$
1-2 ^a	$\varepsilon_\lambda = \exp(a_0 + a_1\lambda + a_2\lambda^2)$	7-1	$\varepsilon_\lambda = \exp(a_0T_\lambda)^c$
1-3 ^a	$\varepsilon_\lambda = \exp(a_0 + a_1\lambda + a_2\lambda^2 + a_3\lambda^3)$	7-2	$\varepsilon_\lambda = \exp(a_0 + a_1T_\lambda)^c$
2-1 ^d	$\varepsilon_\lambda = a_0 + a_1\lambda$	8-1 ^e	$\varepsilon_\lambda = \exp(a_0/T_\lambda)^c$
2-2 ^d	$\varepsilon_\lambda = a_0 + a_1\lambda + a_2\lambda^2$	8-2 ^e	$\varepsilon_\lambda = \exp(a_0 + a_1/T_\lambda)^c$
2-3 ^d	$\varepsilon_\lambda = a_0 + a_1\lambda + a_2\lambda^2 + a_3\lambda^3$	9-1	$\varepsilon_\lambda = \exp(a_0\sqrt{\lambda})$
3 ^f	$\varepsilon_\lambda = 1/(1 + a_0\lambda^2)$	9-2	$\varepsilon_\lambda = \exp(a_0 + a_1\sqrt{\lambda})$
4 ^g	$\varepsilon_\lambda = a_0(T/\lambda)^{1/2}$	10-1	$\varepsilon_\lambda = \exp(a_0/\sqrt{\lambda})$
5 ^b	$\varepsilon_\lambda = \exp(a_0\lambda + a_1T)$	10-2	$\varepsilon_\lambda = \exp(a_0 + a_1/\sqrt{\lambda})$

^a Log-linear emissivity model (LLE).

^b Wavelength temperature emissivity model (WLT).

^c T_λ is spectral radiance temperature defined as equivalent blackbody temperature of measured spectral intensity.

^d Linear emissivity model (LEM).

^e Inverse spectral temperature emissivity model (IST).

^f Inverse wavelength squared emissivity model (IWS).

^g Hagen–Rubens model (HRR).

Section 3.4, the shape of emissivity distribution is fairly pronounced for the polished, 6- and 14- μm surfaces but loses sensitivity to wavelength for extruded and saw-cut surfaces. The 14- μm surface therefore provides an effective basis for assessment of the effectiveness of emissivity models at capturing the pronounced spectral variations for rough surfaces. Thirdly, this roughness was chosen because of its ease of fabrication as well as its statistically uniform and repeatable surface characteristics.

Tables 2 and 3 provide absolute errors in the inferred temperature predicted by the 18 models for surface temperatures of 600 and 700 K, respectively. Values exceeding ± 50 K have been purposely deleted to help point out accurate models and their predictive trends. The results are shown for a relatively short spectral range of 2.05–3.43 μm , a long range of 3.50–4.72 μm , and a combined range of 2.05–4.72 μm . All wavelengths corresponding to the CO_2 and H_2O bands are excluded from the examined wavelength range. Three different numbers of wavelengths, N , $N+1$ and $N+2$ are examined, where N is the required minimum number of wavelengths, $n+2$.

Although Tables 2 and 3 include several cases with absolute error below 1 K, those cases as well as errors below 10 K are somewhat random. Nonetheless, close inspection of temperature errors reveals important trends concerning predictive capability for different spectral ranges, number of wavelengths, number of unknown coefficients in an emissivity model, temperature, and alloy. These trends are used to identify models with the most superior overall predictive capability.

4.1. Effects of spectral range

Tables 2 and 3 show “acceptable results” are concentrated primarily in the combined spectral range (i.e.

2.05–4.72 μm) or in the short range of 2.05–3.43 μm , but not the long range. Therefore, contrary to earlier recommendations [16,17], broadening the wavelength range to encompass all measured wavelengths may not always enhance the predictive capability of an emissivity model. This can be explained by the complex variations of spectral emissivity, and the difficulty of a particular mathematical function at capturing vastly different emissivity trends corresponding to both wavelength ranges.

4.2. Effects of number of wavelengths

Increasing the number of wavelengths used in the spectral measurements is commonly used to facilitate statistical reduction of temperature errors from measurement noise. However, Tables 2 and 3 show the minimum number of wavelengths, N , required by the least-squares MRT technique generally yields satisfactory results, and using a larger number of wavelengths ($N+1$ or $N+2$) does not improve accuracy. This observation is consistent with the findings of previous investigators [17,18].

4.3. Effects of number of unknown coefficients

Excepting a few cases (Models 2-3, 7-2 and 8-2 at 600 K), Tables 2 and 3 show that including additional unknown coefficients do not enhance model accuracy. This finding is consistent with that of Coates [6].

4.4. Effects of temperature

Changes in emissivity spectra due to temperature variations were described earlier in this paper. Further

Table 2
 Absolute error in inferred temperature of aluminum alloy samples roughened with 14 μm grit paper at 600 K

Model	N^a	Wavelength (μm)											
		2.05–3.43				3.50–4.72				2.05–4.72			
		AL 1100	AL 2024	AL 7075	AL 7150	AL 1100	AL 2024	AL 7075	AL 7150	AL 1100	AL 2024	AL 7075	AL 7150
1-1	N		50.0		13.5								
	$N+1$				41.9								
	$N+2$	37.7	8.7		-21.8								
1-2	N												
	$N+1$												
	$N+2$									-15.8	32.8	45.7	
1-3	N												
	$N+1$												
	$N+2$												
2-1	N												
	$N+1$												
	$N+2$												
2-2	N	-42.6	-36.0	-27.5									
	$N+1$			-48.2									
	$N+2$	1.2	-35.0	-11.8		-11.0		-18.1	-12.1				
2-3	N	-5.3	-24.9	-5.0	-28.1	-26.6		22.1		37.7	25.2		29.0
	$N+1$	0.8		-12.2						-22.3		-25.1	
	$N+2$										-4.5		-3.8
3	N	-13.7	-21.2	-8.1	-36.5								
	$N+1$	-5.2	-6.3	3.1	-22.7								
	$N+2$	-4.7	-7.1	-2.8	-23.0								
4	N				24.5								
	$N+1$				44.3								
	$N+2$				45.2								
5	N		39.2		4.8								
	$N+1$		3.9	22.6	32.4		-1.8						
	$N+2$	29.6	1.9	49.1	-16.0		-35.4	39.4					
6	N		42.6		29.5							2.4	
	$N+1$											46.1	
	$N+2$				39.1							3.5	
7-1	N												
	$N+1$												
	$N+2$												
7-2	N	36.3	23.0	44.5	10.7								
	$N+1$	32.1	7.4	39.9	-11.1								
	$N+2$	22.4	0.6	30.0	-16.8								
8-1	N				37.9					28.7	17.7	27.5	11.1
	$N+1$				37.7					28.4	17.0	27.2	11.2
	$N+2$				41.5					28.5	16.6	26.8	10.5
8-2	N		42.6		22.6								
	$N+1$		35.2		6.6								
	$N+2$	39.7	19.7		-3.7								
9-1	N	33.7	31.1	41.9	12.8					3.5	-7.2	1.6	-12.4
	$N+1$	35.2	32.1	43.0	13.0					2.1	-9.7	-0.4	13.5
	$N+2$	36.6	34.5	44.8	16.4					2.1	-10.0	-0.6	-14.1

(continued on next page)

Table 3 (continued)

Model	N^a	Wavelength (μm)												
		2.05–3.43				3.50–4.72				2.05–4.72				
		AL 1100	AL 2024	AL 7075	AL 7150	AL 1100	AL 2024	AL 7075	AL 7150	AL 1100	AL 2024	AL 7075	AL 7150	
5	N									–33.5	33.2			
	$N + 1$		–47.3							3.7	31.5			
	$N + 2$		–32.2		–41.8					32.3	–44.8	40.1		
6	N		–36.1			–49.2				6.0	36.7			
	$N + 1$		44.6	–0.8	26.7			19.0	–37.8		34.5		49.3	
	$N + 2$		2.2		–37.0		3.8	44.5	34.3		38.3			
7-1	N					–3.6		–13.8	–4.2		47.5			
	$N + 1$					–10.6		–18.0	3.5		47.8			
	$N + 2$					4.0		–8.4	–5.9					
7-2	N													
	$N + 1$													
	$N + 2$													
8-1	N	–8.9	2.3	–0.5	–2.9						–24.4	–26.3	–21.9	–24.1
	$N + 1$	–5.7	6.1	3.0	0.2						–24.5	–27.2	–22.3	–24.8
	$N + 2$	–4.5	8.0	4.7	3.3						–23.8	–27.0	–22.0	–24.7
8-2	N													
	$N + 1$			–49.5										
	$N + 2$													
9-1	N	–34.6	–25.1	–27.5	–29.9						–49.2		–47.5	–49.7
	$N + 1$	–31.8	–21.3	–24.1	–26.9						–49.8		–48.6	
	$N + 2$	–30.7	–19.7	–22.7	–24.2						–49.3		–48.3	
9-2	N													
	$N + 1$													
	$N + 2$													
10-1	N													
	$N + 1$													
	$N + 2$													
10-2	N													
	$N + 1$													
	$N + 2$													

Missing values correspond to errors beyond ± 50 K.

^a N is minimum number of wavelengths required in MRT model, which is equal to number of unknown coefficients in model plus two.

insight into the temperature effect can be gained by comparing results from Table 2 to those from Table 3. Both tables show, for most alloys, model 8-1 over the 2.05–4.72 μm and model 9-1 over 2.05–3.43 μm are the most effective at compensating for emissivity variations with temperature.

4.5. Effects of alloy

Applying the appropriate spectral range, and using the required minimum number of wavelengths

($N = n + 2$), models 2-3, 3, 5, 7-2, 8-1, 8-2 and 9-1 at 600 K and 2-1, 2-3, 4, 8-1, 9-1 at 700 K show the best compensation for the different alloys.

In summary, model 1-3 shows the poorest overall compensation for emissivity variations. In contrast, model 8-1 (exponential function of T_j) over 2.05–4.72 μm and model 9-1 (exponential function of $\sqrt{\lambda}$) over 2.50–3.43 μm , show the best overall compensation for different alloys and different temperatures. This is consistent with the authors' earlier findings for polished samples [12].

5. Conclusions

This study explored the effects of temperature, heating time, and surface roughness on spectral emissivity of aluminum alloys. Spectral measurements were performed for several alloys over the range of 2.05–4.72 μm . Eighteen MRT emissivity models were examined for temperature measurement accuracy. Key findings from the study are as follows:

- (1) The emissivity of aluminum samples generally decreases appreciably between 2.05 and 3.5 μm , and increases slightly between 3.5 and 4.72 μm .
- (2) Contrary to the trend of increasing emissivity with increasing temperature for most metallic surfaces, the emissivity of aluminum samples generally decreases between 600 and 700 K and increases between 700 and 800 K. The latter increase is attributed to surface discoloration at 800 K.
- (3) Heating time has a measurable effect on emissivity during the first 4 h of oxidation buildup. Thereafter, the oxidation appears to become fully developed, evidenced by constant emissivity following the initial 4-h period.
- (4) Different alloys generally produce emissivity distributions that are similar in shape but not in magnitude.
- (5) Surface roughness affects spectral emissivity in two ways. In general, the emissivity distribution is very pronounced for the polished, 6- and 14- μm surfaces, and far less pronounced for the highly roughened extruded and saw-cut surfaces. Furthermore, surface roughness generally increases emissivity. This increase is greatest for the saw-cut surface.
- (6) Several of the MRT emissivity models examined in this study provide acceptable results in either the short wavelength range of 2.05–3.43 μm or in the combined range of 2.05–4.72 μm , but not both. This is the result of drastic changes in the emissivity distribution precluding the use of a single function to accurately represent every band of the measured spectrum. It is shown increasing the number of wavelengths above that required by MRT does not improve the predictive capability of an emissivity model. Additionally, using a higher order function of a given emissivity model does not enhance temperature prediction.
- (7) Overall, two relatively simple models, 8-1 (exponential function of $1/T_\lambda$) and 9-1 (exponential of linear first order function of $\sqrt{\lambda}$), provide the best overall compensation for different alloys and different temperatures. These are the same two models that provided the best results for polished aluminum surfaces in a previous study by the authors [12]. Despite the relative success of these two MRT models, this study

points to a need to greatly enhance the measurement accuracy of radiation thermometers to meet the needs of the aluminum industry.

Acknowledgements

Financial support of the Indiana 21st Century Research and Technology Fund is gratefully appreciated. The authors also thank Mr. Gerry Dail of ALCOA for supplying aluminum samples, and Dr. Jongmook Lim of Spectraline for his technical assistance.

References

- [1] Aluminum Facts at a Glance, The Aluminum Association, Washington, DC, 2003.
- [2] G.J. Dail, M.G. Fuhrman, D.P. DeWitt, Evaluation and extension of the spectral-ratio radiation thermometry method, in: Proceedings of 4th International Aluminum Extrusion Technology Seminar, Chicago, IL, 11–14 April 1988, vol. 2, pp. 281–286.
- [3] M.A. Pellerin, Multispectral Radiation Thermometry for Industrial Applications, Ph.D. Thesis, Purdue University, School of Mechanical Engineering, West Lafayette, IN, 1999.
- [4] R. Siegel, J.R. Howell, Thermal Radiation Heat Transfer, McGraw-Hill, New York, 1972.
- [5] D.K. Edwards, I. Catton, Advances in the thermophysical properties at extreme temperatures and pressures, in: Proceedings of Symposium on Thermophysical Properties, Purdue University, West Lafayette, IN, 22–25 March 1965, pp. 189–199.
- [6] P.B. Coates, Multi-wavelength pyrometry, Metrologia 17 (1981) 103–109.
- [7] Y.S. Touloukian, D.P. DeWitt, Thermal radiative properties, metallic elements and alloys, in: Thermophysical Properties of Matter, vol. 7, Plenum Corp., New York, 1970.
- [8] P.M. Reynolds, Spectral emissivity of 99.7% aluminum between 200 and 500 $^{\circ}\text{C}$, Br. J. Appl. Phys. 12 (1961) 111–114.
- [9] M.A. Pellerin, D.P. DeWitt, G.J. Dail, Multispectral radiation thermometry for aluminum alloys, in: Heat Transfer in Metals and Containerless Processing and Manufacturing, vol. HTD-162, ASME, New York, NY, 1991, pp. 43–47.
- [10] M.A. Pellerin, B.K. Tsai, D.P. DeWitt, G.J. Dail, Emissivity compensation method for aluminum alloy temperature determination, in: J.F. Schooley (Ed.), Temperature, its Measurement and Control in Science and Industry, vol. 6, Part 2, American Institute of Physics, New York, 1992, pp. 871–876.
- [11] M.F. Hopkins, Four color pyrometer for metal emissivity characterization, SPIE—The Int. Soc. Opt. Eng. 2599 (1996) 294–301.
- [12] C. Wen, I. Mudawar, Emissivity characteristics of polished aluminum alloys and assessment of multispectral radiation

- thermometry (MRT) emissivity models, *Int. J. Heat Mass Transfer*, in review.
- [13] F.P. Incropera, D.P. DeWitt, *Fundamentals of Heat and Mass Transfer*, fourth ed., John Wiley and Sons, New York, 1996.
- [14] M.J. Haugh, Radiation thermometry in the aluminum industry, in: D.P. DeWitt, G.D. Nutter (Eds.), *Theory and Practice of Radiation Thermometry*, John Wiley and Sons, New York, 1988.
- [15] B.K. Tsai, R.L. Shemaker, D.P. DeWitt, B.A. Cowans, Z. Dardas, W.N. Delgass, G.J. Dail, Dual-wavelength radiation thermometry: emissivity compensation algorithms, *Int. J. Thermophys.* 11 (1990) 269–281.
- [16] J.L. Gardner, Computer modeling of multiwavelength pyrometer for measuring true surface temperature, *High Temp.–High Press.* 12 (1980) 699–705.
- [17] G.R. Gathers, Analysis of multiwavelength pyrometry using nonlinear chi-square fits and Monte Carlo methods, *Int. J. Thermophys.* 13 (1992) 539–554.
- [18] J.L. Gardner, T.P. Jones, M.R. Davies, A six-wavelength radiation pyrometer, *High Temp.–High Press.* 13 (1981) 459–466.